Fabrication of super-hydrophobic copper mesh by liquid oxidation and vapor silylation

X. F. Li*, S. S. Li, L. Zhang
College of Chemical and Materials Engineering of Xuchang University, Xuchang 461000, China

Super-hydrophobic copper mesh was fabricated by liquid oxidation using $K_2S_2O_8$ as oxidant and followed by vapor silylation with hexamethyldisilazane (HMDS). The preparation process was optimized with respect to four factors. The samples were characterized by Water Contact Angle (CA), XRD, FTIR, respectively as well as evaluated by oil-water separation test. The obtained optimum preparation condition is a $K_2S_2O_8$ concentration of 0.145 mol·L^{-1}, a oxidation time of 60 min, a calcaination temperature of 300 °C and a silylation temperature of 190 °C, under which the highest CA can achieve 154°. XRD and FTIR characterizations demonstrate the reaction result of the oxidation of CM to form OCM and of the silylation of OCM to form SOCM, respectively. CM, OCM and SOCM are shown to be low hydrophobicity, hydrophilicity and high hydrophobicity (CA = 154°), respectively. Three samples possess a oil-water (methylbenzene-water) separation ratio of 45.6%, 3.3% and 99.9%, respectively. The reusing experiments for methylbenzene, chloroform and kerosene indicate that SOCM can be utilized for 30 cycles and retains an oil-water separation efficiency of at least 98% for any one oil. It suggests that SOCM has an excellent hydrophobicity, which results from the vapor silylation as a vesatile method for modifying the copper mesh.

(Received January 26, 2023; Accepted April 24, 2023)

Keywords: Copper mesh, Liquid oxidation, Vapor silylation, Super-hydrophobicity, Oil-water separation

1. Introduction

In the past decades, the expanding water pollution has seriously threatened the human health and ecological environment. The pollution cases were mainly from the frequent oil spill accidents, as well as ever-increasing industrial oily wastewater discharge [1]. For example, in 2010, the explosion of BP's Deepwater Horizon oil rig resulted in 210 million gallons of crude oil being released into the Gulf of Mexico [2]. The cost of the oil spill, including the damage to the coastal ecosystem and the loss of an entire fishing and tourism season, is still being tabulated [3]. Especially, the failure to prevent crude oil from reaching sensitive areas increased damages and drew widespread public attention. Accordingly, the need for new technological approaches to oil spill remediation is highly desired.

* Corresponding author: snow_mount@163.com
https://doi.org/10.15251/DJNB.2023.182.627

In general, traditional techniques including floating [4], adsorption [5], in situ burning [6], biological treatment [7], chemical oxidation [8], and chemical degradation [9] have been widely used for handling oil spills. However, any one method still has more or less disadvantages such as high cost, low separation efficiency, and/or secondary pollutant production [1]. Therefore, it is of great importance to develop novel means or advanced materials to separate oil-water mixtures in a selective, highly-efficient, and green manner.

Recent years, oil-water separation with superhydrophobic materials as an effective method to treat wastewater has been paid much more attention. This technique is often preferred because it allows for the proper disposal of oil and does not cause secondary pollution [10]. The first excellent example of oil-water separation was being reported by Jiang et al. using a mesh coated with hydrophobic and oleophilic materials [11]. Following this work, the removal of oil from water by hydrophobically modified, oil-selective meshes had been reported several times previously [12-18]. In these literature, the use of superhydrophobic meshes have been shown to create efficient separation of water–oil mixtures by allowing oils to fall through the pores in the mesh whilst retaining the water on the surface. It has been demonstrated that superhydrophobic effect comes from the combination of a special rough structure and lower surface energy on such surfaces. To achieve a superhydrophobic surface, two conditions, namely low surface energy [19] and higher roughness [20], must be satisfied [21]. In the case of higher roughness, several techniques including top down approaches such as lithography, templating, and micromachining and bottom up approaches such as chemical deposition assemblies of colloids, layer by layer methods, and electrospinning, have been reported for improving the roughness to fabricate the superhydrophobic surface [20,21]. However, most of these techniques require expensive chemicals, harsh conditions, multifabrication steps, or special equipment [21]. Comparatively speaking, the method by grafting the particular materials with low surface energy onto the mesh surface is simple, involves minimal steps, and is cost-effective for preparing superhydrophobic surfaces [21]. In the previous literature, poly dimethylsiloxane (PDMS) and fluorinated silanes were utilized to reduce the surface energy [1,22].

However, fluorinated compounds have also been identified as a source of toxic pollutants which persist in the environment [23]. PDMS has been considered as an environmentally friendly grafting agent, but considerable $CH_3Si(OH)_2$ groups will not completely react with the surface active sites, which leads to remain hydrophilic Si-OH groups and decrease the hydrophobicity [1,21]. Therefore, it is necessary to develop a preferred technique that can obtain the hydrophobic surface by an both easy and cost-effective method as well as using green agents.

In the present work, a super-hydrophobic copper mesh was prepared via oxidation by $K_2S_2O_8$ and vapor silylation of HMDS. We also systematically explored the influence of oxidation and silylation conditions on the contact angle of the mesh surface to optimize the preparation process. The super hydrophobic mesh surface was obtained and exhibited an excellent performance in oil-water separation.

2. Experimental

2.1. Materials

Copper mesh (200 mesh size, AR) was purchased from Anping County Bolin Wire Mesh Co., Ltd. Potassium persulfate ($K_2S_2O_8$, AR) was purchased from Tianjin Kaitong Chemical Agent Co., Ltd. Hydrochloric acid (HCl, AR) was supplied by Luoyang Haohua Chemical Agent Co., Ltd. Sodium hydroxide (NaOH, AR), Absolute alcohol (EtOH, AR) and Hexamethyl disilylamine (HMDS, AR) are supplied by Sinopharm Chemical Reagent Co., Ltd. Deionized water (H_2O, AR) was prepared by Xuchang University.

2.2. Sample preparation

2.2.1. Pretreatment of copper mesh

Copper mesh was cut into many pieces (1cm × 3cm), and subsequent ultrasonically cleaned with hydrochloric acid solution (0.10 mol·L^{-1}, 30 min), absolute ethanol (30 min), and deionized water (30 min), respectively to remove the surface dirt and finally dried in the air. The obtained mesh was denoted as CM and stored in a desiccator for the following use.

2.2.2. Oxidation and calcination of copper mesh

CM was put into a mixture solution consisting of $K_2S_2O_8$ (0.065 to 0.185 mol·L^{-1}) and NaOH (4.50 mol·L^{-1}) in water [24]. A water bath was utilized to control the solution temperature. The oxidation reaction was carried out at 60 ℃within a defined time (15 to 75 min). The oxidized copper mesh was washed with water, dried in the air and calcinated at a specified temperature (from 150 to 350 ℃) for 2 h. After calcination, the obtained copper mesh was denoted as OCM.

2.2.3. Vapor silylation of copper mesh

The vapor silylation process was carried out on a quartz tube reactor. The typical procedure is as follows [25]. Firstly, OCM was put into a quartz tube and nitrogen flow (150 ml/min) was passed through the OCM mesh holes at 200 °C for 2 h. After this nitrogen treatment, OCM reacted with the HMDS vapor in nitrogen flow at a defined temerature (130~250 °C) for 2 h. Finally, the silylated OCM was washed and dried using nitrogen flow at 150 °C for 2 h. The obtained copper mesh was final product and denoted as SOCM.

2.3. Characterization of samples

The X-ray diffraction (XRD) analysis was conducted using an X-ray diffractometer (X' pert Pro MPD, Netherlands) with Cu Kα radiation. Fourier transform infrared (FT-IR) spectra were obtained by a FT-IR spectrometer (Vector 33, Germany). The surface morphologies of as-prepared copper mesh samples were observed by a scanning electronic microscope (SEM, EVOLS-15) from Zeiss company in Germany.

2.4. Hydrophobicity test

2.4.1. Water contact angle

The water contact angle (CA) value was measured at ambient temperature by a contact angle measurement instrument (C60, USA KINO) equipped with a high speed video camera. For each CA measurement in the air, a water droplet of 3 μL was directly placed on the sample surface

in the air using a micro-syringe. Three measurements were made using three drops of water at three different spots on each sample. The final CA value of each sample was the mean of three measurements.

2.4.2. Oil-water separation

The as-prepared copper mesh was fixed between two glass tubes, reinforced by a stainless steel clip. Three oils including methylbenzene, chloroform and kerosene were used in this study. The selected oil was mixed with deionized water (stained with methylene blue). The oil-water mixture (50 mL) was poured into a test tube after the mesh prewetted by water. The separation process was recorded by a digital camera built-in a mobile phone (Huawei, China). The oil-water separation efficiency (*E*) was defined to be the mass ratio of the selected oil after and before separation.

The oil-water separation reusability of mesh sample was evaluated with five same experiments. In a typical resue case, the five separation tests were consecutively taken and the accumulative mixture (250 mL) was collected. The oil-water separation efficiency (*E*) was calculated based on the above-mentioned definition [1].

3. Results and discussions

3.1. Preparation

3.1.1. Concentration of $K_2S_2O_8$ in solution

The experiments were carried out to investigate the effect of $K_2S_2O_8$ concentration in solution on the CA value of the final copper mesh sample [24]. The concentrations of $K_2S_2O_8$ range from 0.065 to 0.185 mol·L^{-1} with a step of 0.02 mol·L^{-1}. The other parameters are fixed as 4.5 mol·L^{-1} of NaOH concentration, 45 min of oxidation time, 250 °C of calcination temperature and 190 °C of silylation temperature, respectively. The results are displyed in Fig. 1. At the lowest concentration of 0.065 mol·L^{-1}, the CA value is 140°. Then, the CA value increases with increasing the concentration of $K_2S_2O_8$ and reaches a maximum of 153° at that of 0.145 mol·L^{-1}. Obviously, this law can be explained by the fact that high concentration $K_2S_2O_8$ will lead to produce more $Cu(OH)_2$ species, which can graft more trimethylsil groups (-Si-$(CH_3)_3$) to enhance the surface hydrophobicity of copper mesh. The surface reactions may be illustrated as in equations (1), (2) and (3) [26].

$$Cu+2NaOH+K_2S_2O_8 \rightarrow Cu(OH)_2\text{（blue）}+K_2SO_4+Na_2SO_4 \quad (1)$$

$$Cu+NaOH+0.5K_2S_2O_8 \rightarrow CuOH+0.5K_2SO_4+0.5Na_2SO_4 \quad (2)$$

$$2Cu\text{-}OH + HDMS \rightarrow 2Cu\text{-}O\text{-}Si(CH_3)_3 \quad (3)$$

However, the CA value declines after the concentration of $K_2S_2O_8$ being beyond 0.145 mol·L^{-1}. It is because that higher $K_2S_2O_8$ concentration results in the transformation of $Cu(OH)_2$ to Cu_2O and make fewer Cu-OH species react with trimethylsil to reduce the surface hydrophobicity.

The following equations (4) and (5) can describe the above mentioned results and mechanism.

$$Cu(OH)_2 \rightarrow CuO\ (black) + H_2O \quad (4)$$

$$CuOH \rightarrow 0.5Cu_2O + 0.5H_2O \quad (5)$$

Meanwhile, during the oxidation reaction, we find the solution becoming baby blue and copper mesh changing from yellow to black. This phenomenon also confirms the corresponding inference reaction with regards to the results and mechanism.

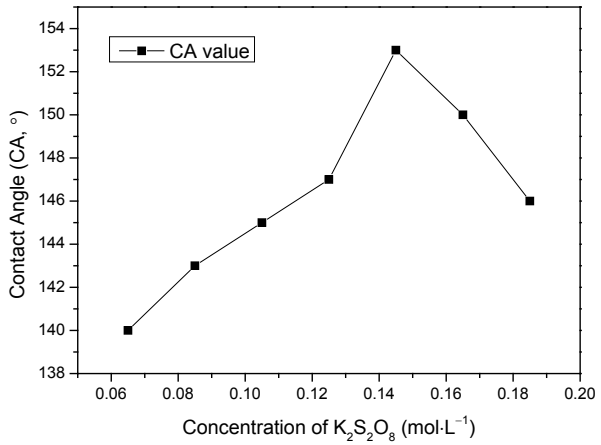

Fig. 1. Relationship between the CA value and the concentration of $K_2S_2O_8$ solution.

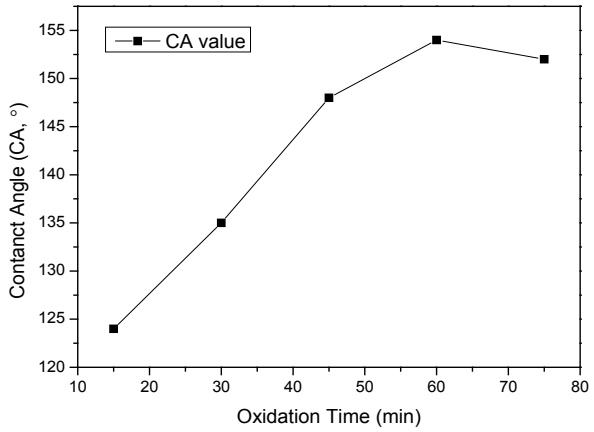

Fig. 2. Relationship between the CA value and the CM oxidation time.

3.1.2. Time of oxidation treatment

The second groups of experiments for optimizing the oxidation time were conducted under a condition of 4.5 mol·L^{-1} of NaOH concentration, a $K_2S_2O_8$ concentration of 0.145 mol·L^{-1}, a changed oxidation time from 15 to 75 min, a calcination temperature of 250 °C and a silylation temperature of 190 °C. As shown in Fig. 2, the CA value increases with increasing oxidation time and reaches 154° as a top value at 60 min. However, it decreases with continuing the increase of

the oxidation time beyond 60 min. As a result, 60 min is an best oxidation time, for which the highest CA value reaches 154°. The reason for the result may be that the oxidation treatment can affect the production of Cu-OH species, which accord with the explanation for the effect of the concentration of $K_2S_2O_8$ in solution.

3.1.3. Temperature of calcination

As we all know, the purpose of the calcination treatment is to control the concentration and distribution of Cu-OH species and ultimately improve the surface hydrophobicity by increasing the grafted trimethylsil quantity. In order to afford an appropriate surface to facilitate vapor silylation reaction, the copper mesh after oxidaiton was calcined at 150~350 °C. Meanwhile, the other parameters were kept as 4.5 $mol \cdot L^{-1}$ of NaOH concentration, 60 min of oxidation time and 190 °C of silylation temperature, respectively. Fig. 3 displays the effect of the calcination temperature on the CA value of the final copper mesh. The result shows that the CA value increases at low calcination temperatures while decreases at high temperatures and reaches a top value of 154° at 300 °C. It may be because that the calcination at higer temperature (but not beyond 300°C) can result in more Cu-OH species, however, the calcination at the temprature beyond 300 °C might lead to form more CuOCu species and to reduce Cu-OH ones.

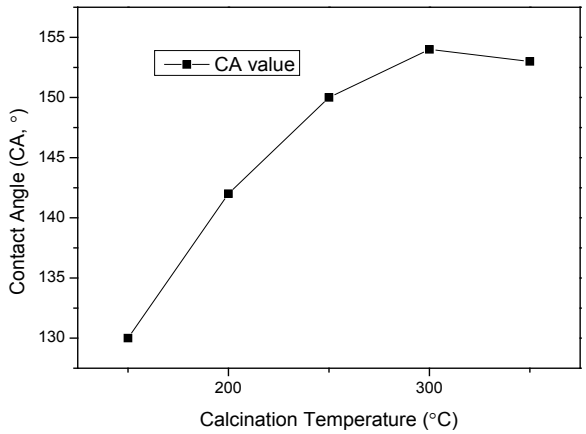

Fig. 3. Relationship between the CA value and the calcination temperature.

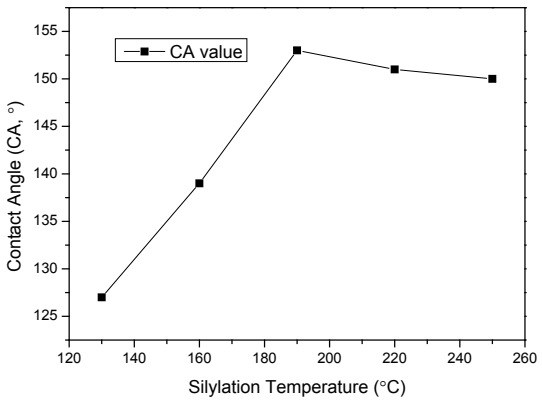

Fig. 4. Relationship between the CA value and the vapor silylation temperature.

3.1.4 Temperature of vapor silylation

Among the preparation steps, vapor silylation of HMDS on copper mesh is an significant procedure. Generally, three factors, namely temperature, time and HMDS concentration, play important roles in affecting the silylation efficiency [25]. For instance, a long silylation time (e.g 2h) or a high HMDS concentration can afford an excess HMDS dosage to achieve a thorough silylation reaction. Accordingly, silylation temperature become a crucial factor and worth optimizing. As shown in Fig. 4, the changing law of the CA value with the temperature of vapor ilylation is as analogous as that with other thee factors. The CA value increases with temperature at low silylation temperatures while decrease after the temperature above the top of 190 °C. It can be evidenced by the fact that Cu-OH reacts with HDMS to form Cu-O-Si$(CH)_3$ as shown in the equation (3) at the temperatures ranging from 130 to 190 °C. However, at high temperatures beyond 190 °C, HDMS will decompose to produce SiO_2, NO_x and CO_x, which discharge taken by the nitrogen flow. Accodingly, higher temperature reduces the silylation efficiency.

3.2. Characterization

3.2.1. XRD

Fig.5 displays XRD patterns of CM, OCM and SOCM, respectively. CM exhibits an intense peak at $2\theta = 43°$, two moderately intense peaks at $2\theta = 50°$ and 73°, ascribed to (111), (200) and (220) lattice planes of Cu, respectively. OCM and SOCM retain the three characteristic peaks besides appearing two newly weak peaks at $2\theta = 36°$ and 39°, assigned to (002) and (100) lattice planes of CuO, respectively [26,27]. It suggests the real occurrence of the oxidation reaction and the absence of damage to CuO crystalline phase by silylation reaction. Meanwhile, the peak intensity of SOCM is slightly lower than that of OCM. It is maybe owing to the fact that the silylation reaction reduces the concentration of Cu-O species.

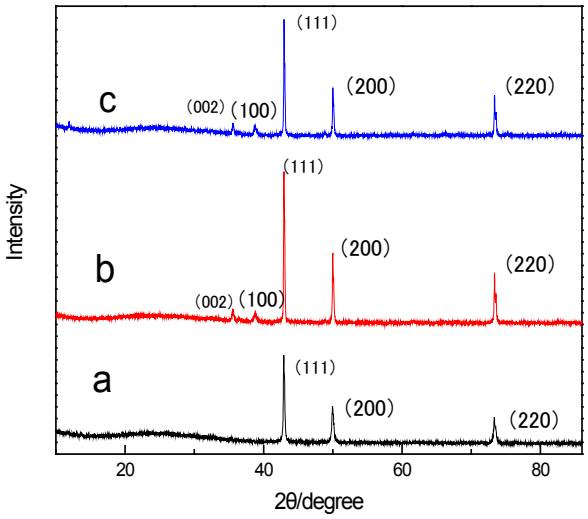

Fig. 5. XRD patterns of CM (a), OCM (b) and SOCM (c).

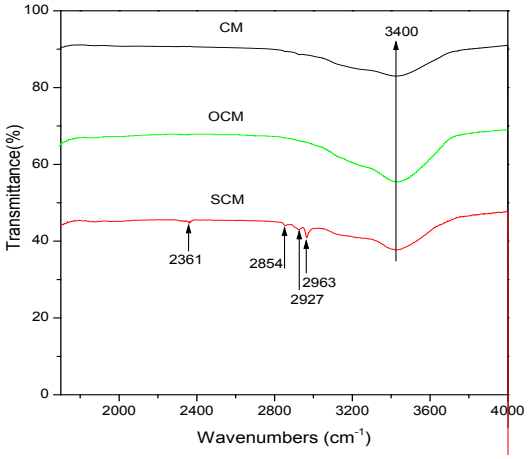

Fig. 6. FTIR spectra of CM, OCM and SOCM.

3.2.2. FTIR

As shown in Fig. 6, a groups of FTIR spectra of CM, OCM and SOCM express a clear evidence of the presence or absence of surface species. CM and OCM exhibit two analogous spectra except the peak at 3400 cm^{-1} of OCM is broader and stronger that of CM maybe due to the presence of more OH groups in OCM surface. Obviously, SOCM gives four peaks at 2361, 2854, 2927 and 2963 cm^{-1} asssigned to stretch vibration of Si-C bond and C-H bond [18]. Meanwhile, most of the Cu-O species peaks are weakened. It is justified that the silylation reaction has been introduced the trimethylsil group onto the OCM surface and most Cu-OH species have been transformed to Cu-OSi$(CH_3)_3$ groups.

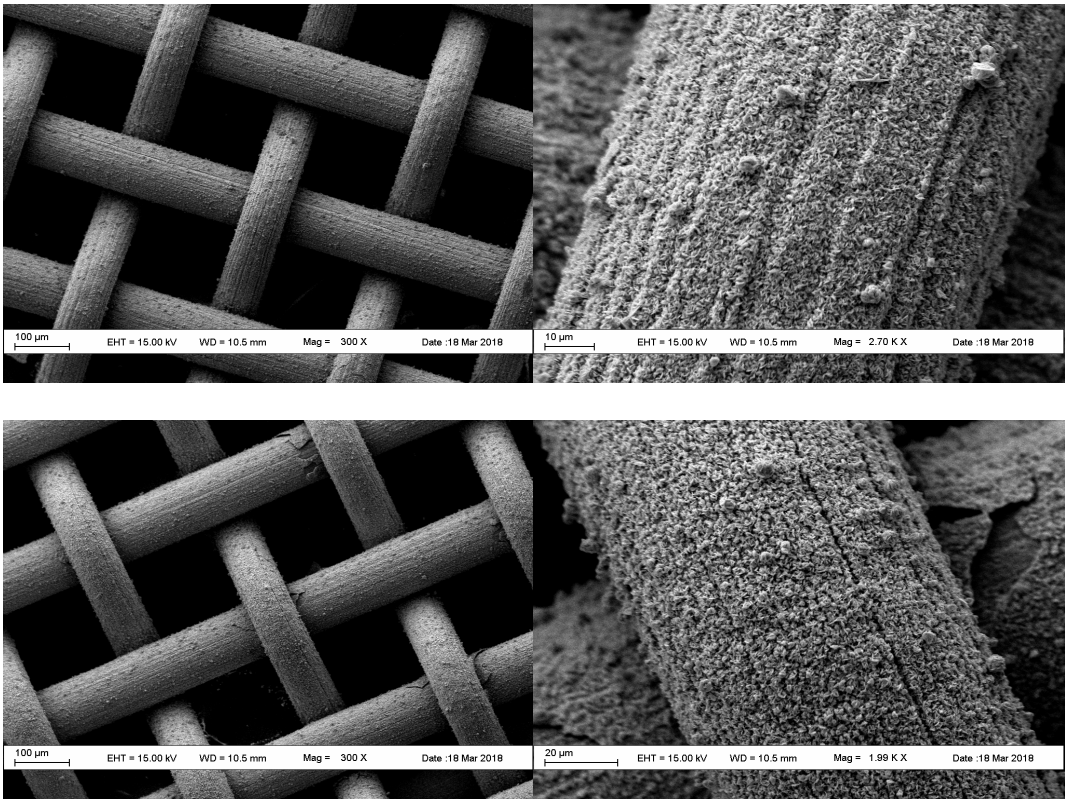

Fig. 7. SEM emages of OCM (upper, left 300×, right 2700×) and SOCM (lower, left 300×, right 1990×).

3.2.3. SEM

SEM images in Fig. 7 show that OCM and SOCM almost have same surface morphologies. Both of two surfaces display tiny sharp bulges and some lumps. It suggests that the silylation treatment does not significantly affect the surface appearance of OCM. The result also indicates that the hydrophobicity of SOCM does not originate from the surface micro-nano structure but originates from the $OSi(CH_3)_3$ groups after silylation reaction.

Fig. 8. The surface wetting illustration and the corresponding CA value of CM (a), OCM (b) and SOCM (c), respectively.

3.3. Hydrophobicity test

3.3.1. Water contact angle

Fig. 8 presents the CA test results of CM, OCM and SOCM, respectively. Apparently, the water droping onto CM surface turns into a flat one, which indicates the CA value is less than 90°. In the case of OCM, the surface is soaked and the water drop immediately spreads showing a CA of almost 0°. However, when using SOCM as test sample, the form of the water drop hardly change and as a result, the measured CA reaches 154°. It suggests a hydrophobicity sequence of SOCM > CM > OCM. The findings can be explained that Cu-OH species resulting from oxidation treatment makes OCM surface hydrophilic and trimethylsil groups arising from vapor deposition dramatically boosts the hydophobicity of SOCM.

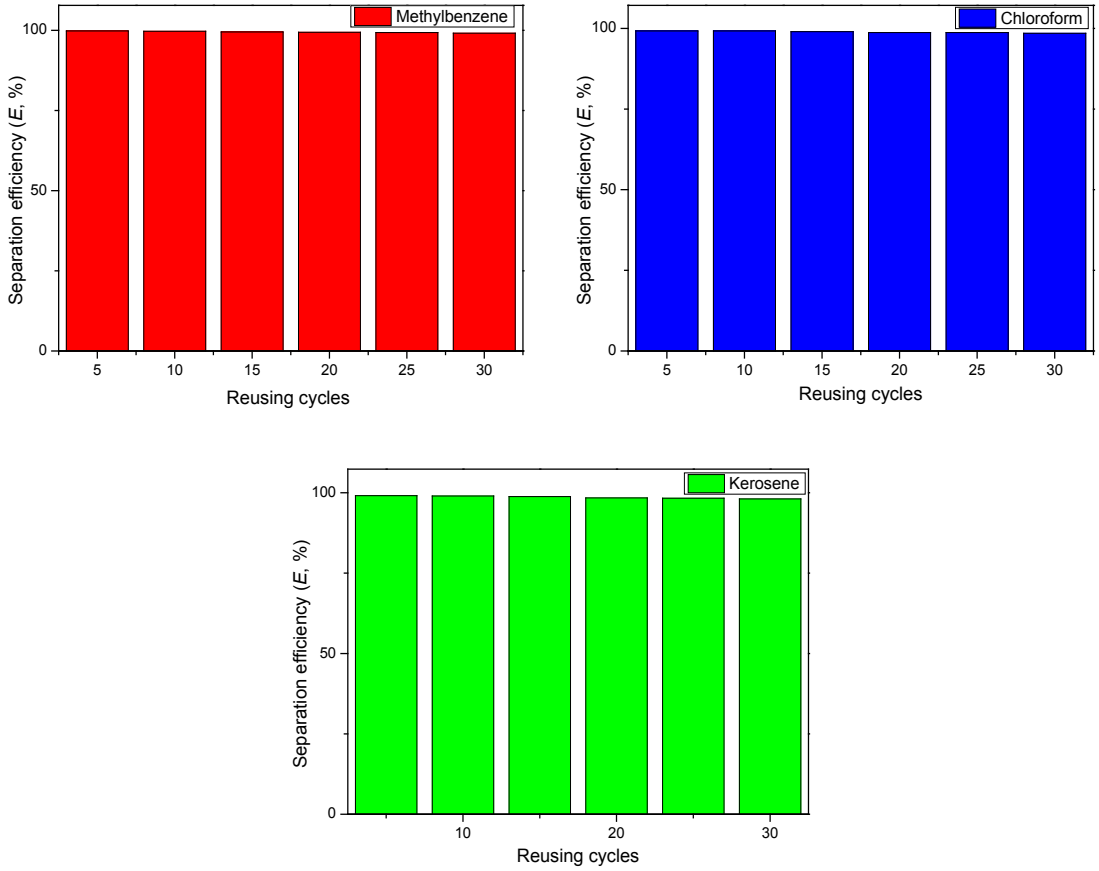

Fig. 9. The SOCM reusing performance for oil-water separation within 30 cycles.

3.3.2. Oil-water separation

Firstly, methylbenzene-water mixture was taken as the test object for the oil-water separation. The measured oil-water separation efficiency of CM, OCM and SOCM are 45.6%, 3.3% and 99.9%, respectively, which accords with the above mentioned CA results. To further evaluate the separation performance of the as-prepared meshes, the separation efficiency for methylbenzene, chloroform and kerosene with 30 reusing cycles were determined as shown in Fig. 9. The efficiency for methylbenzene, chloroform and kerosene slowly decines from 99.8% to 99.1%, 99.2% to 98.5% and 99.1% to 98.1%, respectively. The minute differences among them may origin from the different oil polarity. In all of three cases, every separation efficiency is still kept in a high level (~98%) until 30 cycles.

4. Conclusions

The water contact angle (CA) of each copper mesh sample increases with increasing the $K_2S_2O_8$ concentration, the oxidation time the calcination temperature and silylation temperature, respectively, and reaches a top value while the CA value decrease with continuing the increment of each factor. The obtained optimum preparation condition is a $K_2S_2O_8$ concentration of 0.145

mol·L^{-1}, a oxidation time of 60 min, a calcaination temperature of 300 °C and a silylation temperature of 190°C, under which the highest CA can achieve 154°. XRD and FTIR characterizations demonstrate the reaction result of the oxidation of CM to form OCM and of the silylation of OCM to form SOCM, respectively. CM, OCM and SOCM are shown to have low hydrophobicity, hydrophilicity and high hydrophobicity (CA = 154°), respectively. Three samples possess a oil-water separation ratio of 45.6%, 3.3% and 99.9%, respectively. The reusing experiments for methylbenzene, chloroform and kerosene indicate that SOCM can be utilized for 30 cycles and retains an oil-water separation efficiency of at least 98% for any one oil. It suggests that the SOCM has an excellent hydrophobicity, which results from the vapor silylation as a vesatile method for modifying the copper mesh.

Acknowledgements

Thanks for the Overseas students science and technology activities project merit funding in Henan Province (202115).

References

[1] Wen N., Miao X., Yang X., Long M., Deng W., Zhou Q., and Deng W., Sep. Purif. Technol., 2018, 204, pp. 116-126; https://doi.org/10.1016/j.seppur.2018.04.059

[2] Wang, C.-F., and Lin, S.-J., ACS Appl. Mater. Interfaces, 2013, 5(18), pp. 8861; https://doi.org/10.1021/am403266v

[3] Deng, D., Prendergast, D.P., MacFarlane, J., Bagatin, R., Francesco, S., and Gschwend, P.M., ACS Appl. Mater. Interfaces 2013, 5(3), pp. 774−781; https://doi.org/10.1021/am302338x

[4] Santo, C.E., Vilar, V.J.P., Botelho, C.M.S., Bhatnagar, A., Kumar, E., and Rui, A.R.B., Chem. Eng. J., 2012, 183, pp. 117-123; https://doi.org/10.1016/j.cej.2011.12.041

[5] Zhu, Q., Pan, Q., and Liu, F., J. Phys. Chem. C, 2011, 115, pp. 17464-17470; https://doi.org/10.1021/jp2043027

[6] Fritt-Rasmussen, J., Wegeberg, S., and Gustavson, K., Water Air Soil Pollut., 2015, 226(10), Article: 329; https://doi.org/10.1007/s11270-015-2593-1

[7] Toor, S.S., Rosendahl, L., and Rudolf, A., Energy, 2011, 36, pp. 2328-2342; https://doi.org/10.1016/j.energy.2011.03.013

[8] Abdelwahab, O., Amin, N.K., El-Ashtoukhy, E.S.Z., J. Hazard. Mater., 2009, 163, pp. 711-716; https://doi.org/10.1016/j.jhazmat.2008.07.016

[9] Kleindienst, S., Paul, J.H., Joye, S.B., Nat. Rev. Microbiol., 2015, 13, pp. 388-396; https://doi.org/10.1038/nrmicro3452

[10] Choi, S.-J., Kwon, T.-H., Im, H., Moon, D.-I., Baek, D.J., Seol, M.-L., Duarte, J.P., and Choi, Y.-K., ACS Appl. Mater. Interfaces, 2011, 3, pp. 4552-4556; https://doi.org/10.1021/am201352w

[11] Feng, L., Zhang, Z., Mai, Z., Liu, B., Jiang, L., and Zhu, D., Angew. Chem., Int. Ed., 2004, 43, pp. 2012-2014; https://doi.org/10.1002/anie.200353381

[12] Wang, S.T., Song, Y.L., and Jiang, L., Nanotechnology, 2007, vol. 18, no. 1, Article: 015103;

https://doi.org/10.1088/0957-4484/18/1/015103

[13] Wang, C., Yao, T., Wu, J., Ma, C., Fan, Z., Wang, Z., Cheng, Y., Lin, Q., and Yang, B., ACS Appl. Mater. Interfaces, 2009, 1(11), pp. 2613-2617; https://doi.org/10.1021/am900520z

[14] Wu, J., Chen, J., Qasim, K., Xia, J., Lei, W., and Wang, B.P., J. Chem. Technol. Biotechnol., 2012, 87, (3), pp. 427-430; https://doi.org/10.1002/jctb.2746

[15] Deng, X., Shang, J., Wang, Z., Shi, H., Zhang, J., Su, X., Xie, Q., and Ma, M., Chin. J. Appl. Chem., 2013, 30, (7), pp. 826-833; https://doi.org/10.3724/SP.J.1095.2013.20437

[16] Ren, G., Song, Y., Li, X., Zhou, Y., Zhang, Z., Zhu, X., Appl. Surf. Sci., 2018, 428(15), pp.520-525; https://doi.org/10.1016/j.apsusc.2017.09.140

[17] Cao, Y., Zhang, X., Tao, L., Li, K., Xue, Z., Feng, L., and Wei, Y., ACS Appl. Mater. Interfaces, 2013, 5(10), pp. 4438-4442; https://doi.org/10.1021/am4008598

[18] Kong, L.-H., Chen, X.-H., Yu, L.-G., Wu, Z.-S., and Zhang, P.-Y., ACS Appl. Mater. Interfaces, 2015, 7, pp. 2616−2625; https://doi.org/10.1021/am507620s

[19] Blossey, R., Nat. Mater., 2003, 2(5), pp. 301−306; https://doi.org/10.1038/nmat856

[20] Verho, T., Bower, C., Andrew, P., Franssila, S., Ikkala, O., Ras, R.H.A., Adv. Mater., 2011, 23(5), pp. 673−678; https://doi.org/10.1002/adma.201003129

[21] Iqbal, R., Majhy, B., and Sen, A.K., ACS Appl. Mater. Interfaces, 2017, 9(36), pp. 31170−31180; https://doi.org/10.1021/acsami.7b09708

[22] Liu, X., Xu, Y., Chen, Z., Ben, K., Guan, Z., RSC Adv., 2015, 5, pp. 1315−1318; https://doi.org/10.1039/C4RA12850H

[23] Russell, M.H. Berti, W.R., Szostek, B., Buck, R.C., Environ. Sci. Technol., 2008, 42(3), pp. 800−807; https://doi.org/10.1021/es0710499

[24] Pan, Q., Wang, M., Wang, H., Appl. Surf. Sci., 2008, 254(18), pp. 6002−6006; https://doi.org/10.1016/j.apsusc.2008.03.034

[25] Li, X., J. Sol-Gel Sci. Technol., 2015, 76(3), pp. 476−481; https://doi.org/10.1007/s10971-015-3796-z

[26] Khedir, K.R., Saifaldeen, Z.S., Demirkan, T.M., Al-Hilo, A.A., Brozak, M.P., Karabacak, T., Adv. Eng. Mater., 2015, 17(7), 982−989; https://doi.org/10.1002/adem.201400397

[27] Hassan, I.A., Parkin, I.P., Nair S.P., and Carmalt, C.J., J. Mater. Chem. B, 2014, 2, 2855−2860; https://doi.org/10.1039/C4TB00196F